

Journal of Materials Chemistry A

Accepted Manuscript



This is an *Accepted Manuscript*, which has been through the Royal Society of Chemistry peer review process and has been accepted for publication.

Accepted Manuscripts are published online shortly after acceptance, before technical editing, formatting and proof reading. Using this free service, authors can make their results available to the community, in citable form, before we publish the edited article. We will replace this *Accepted Manuscript* with the edited and formatted *Advance Article* as soon as it is available.

You can find more information about *Accepted Manuscripts* in the [Information for Authors](#).

Please note that technical editing may introduce minor changes to the text and/or graphics, which may alter content. The journal's standard [Terms & Conditions](#) and the [Ethical guidelines](#) still apply. In no event shall the Royal Society of Chemistry be held responsible for any errors or omissions in this *Accepted Manuscript* or any consequences arising from the use of any information it contains.

Fabrication of textile fabric counter electrode using activated charcoal doped multi walled carbon nanotube hybrid for dye sensitized solar cell

Alvira Ayoub Arbab^a, Kyung Chul Sun^b, Iftikhar Ali Sahito^a, Anam Ali Memon^a, Yun Seon Choi^a, Sung Hoon Jeong^{a*}

^aDepartment of Organic and Nano Engineering, Hanyang University, Seoul 133-791, Korea

^bDepartment of Fuel cells and hydrogen technology, Hanyang University, Seoul 133-791, Korea

*Email:shjeong@hanyang.ac.kr

Abstract

Textile fabric electrodes have attained increasing demand as they offer the benefits of light weight, flexibility, and low cost. In this work, we fabricated an activated charcoal doped multi walled carbon nanotube (AC doped MWCNT) hybrid and printed on polyester woven fabric. This carbon fabric composite used as counter electrode (CE) in dye sensitized solar cell (DSSCs), so as to replace expensive platinized FTO (fluorinated tin oxide) glass. Variety of mesoporous carbon structures were synthesized by using different types of charcoal together with MWCNT. Morphological characterization revealed that the highly porous defect rich carbon structure consists of synchronized features of 3D carbon decorated with MWCNT network. The excessive oxygen surface groups can reduce large amount of polymer gel electrolyte and locates manifold catalytic sites for reduction of tri-iodide (I_3^-). Electrochemical investigations confirmed that this carbon fabric composite has high electro catalytic activity (ECA) and exhibited very low charge transfer resistance (R_{CT}) of 1.38 Ω . The resulting N719 DSSCs consist of this unique carbon coated textile fabric CE filled with polymeric electrolyte show power conversion efficiency (PCE) of 7.29%, outperforming platinized FTO glass CE.

Such facile assembly of this novel textile fabric CE is quite promising for the mass production of next generation textile structured solar cell.

1. Introduction

Textile based electrode have received much attention due to their potential application in super capacitor,¹⁻⁴ lithium ion batteries,⁵⁻⁷ and electrochemical energy storage devices.⁸⁻¹⁰ These electronic textiles (e-textiles) offer the combined features of light weight, flexibility and charge storage capacity.¹¹⁻¹⁵ In photovoltaic devices, dye sensitized solar cells (DSSCs) have received much attention due to their low cost, high sustainability, and easy fabrication.¹⁶⁻¹⁸ A standard DSSC consist of an n-type TiO_2 nano crystalline semiconductor oxide particulates as anode electrode, platinized FTO glass as cathode separated with a I^-/I_3^- redox couples electrolyte. Typical DSSCs suffer from stability problems that result from their use of platinized fluorinated tin oxide (FTO) glass cause low sustainability.¹⁹ However, commercial application of platinized CE is restricted by its high cost and high energy consuming preparation (sputtering and thermal decomposition). Consequently, extensive research has been carried out for the progress of platinized FTO free CE in DSSCs. Recently, fabrication of flexible carbon fabric composites have gained widespread attention due to their high conductivity, low cost, and environmental sustainability. Design and fabrication of micro and nano-patterned carbon structures based on carbon nanotubes, carbon black, graphite, and graphene has been assembled on fabric substrate and used as efficient CE substrate.²⁰⁻²⁶

Multi walled carbon nanotubes (MWCNTs) are a unique nano scale structure, consist of several coaxially arranged graphene sheets with distinct electronic features of high electrical conductivity, and chemical stability. MWCNTs are made up of nearly perfect atomically smooth basal planes which may not be suitable for efficient electro-catalytic application.²⁷ Amorphous

activated charcoal has high surface area with porous structure, possess multi-edges surface that can act as active centers for the charge storage reactions.^{28,29} Induction of mesoporous activated carbon into the tubular graphitic framework without alter their electronic conductivity could yield electro catalytic active sites with minimum change of conjugation length. Synchronized structure of defect rich carbon with conductive MWCNT network supports to facilitate the charge transfer kinetics, and improve the device photovoltaic efficiency.

Textile fabrics are porous and stretchable made by weaving, knitting, or pressing fibers. Among the fabrics, polyester fabric is indeed the most commonly used because of its high strength, flexibility, and low production cost. In this paper, we report a novel textile fabric CE employing a polyester fabric as substrate, and AC doped MWCNT as catalytic coating, which is synthesized by enzymatic dispersion route, reported in our previous work.³⁰ We fabricated different composite structures of AC doped MWCNT printed polyester fabric (carbon fabric composites) using coal, coconut shell and pine tree type activated carbon, designated as composite A, composite B and Composite C, respectively. Further, different amounts of AC (pine tree) were formulated to optimize hybrid structure. Electrochemical studies revealed the high electro catalytic activity and conductivity of our suggested textile CE. Further, DSSCs were fabricated with FTO based anodes and carbon fabric composite CEs. Polyethylene oxide based gel electrolyte was used to avoid the electrolyte leakage. The initial photovoltaic results showed that, the carbon fabric composite prepared with 0.8% AC, exhibited high photovoltaic performance with 7.29% efficiency, outperforming platinized FTO with 7.16% PCE. The achieved PCE is among the highly efficient N719 DSSCs using fabric based CEs. In flexible CEs, it was mainly the V_{OC} and FF among photovoltaic parameters that affect the efficiency of device. Briefly, the higher FF and V_{OC} of our suggested carbon fabric composite attributed to the

strong adhesion of carbon layer with textile substrate, better sheet conductivity, and lower interfacial charge transfer resistance with polymer gel electrolyte.

In addition to replacing Pt with AC doped MWCNT as the electro catalyst, the FTO substrate for CE was also replaced by woven fabric to further reduce the cell internal resistance and thus improve cell efficiency. Textile CE based DSSCs are expected to meet the various requirements of wearable electronics. These highly conductive and electro catalytic active electrodes can be further fabricated into flexible transparent conductive glass (TCO) free DSSCs. In addition, the production of fabric based composites are very mature in textile industries, can provide benefit of roll-to roll production of flexible TCO free DSSCs.

2. Experimental

2.1 Materials

Plain weave 100 % polyester fabrics, with silicon hydrophobic surface finish were used as substrate. Three types of activated charcoal particles derived from coal, coconut shell and pine tree were purchased from Dy-carbon Co. MWCNT powder of carbon content > 95 %, 6-9 nm diameter, 5 μ m length (Sigma Aldrich Co.) was used. Lipase enzyme from candida rugosa, Type VII (Sigma Aldrich Co.) used as organic dispersant. Polymer carboxymethyl cellulose (sodium salt of MW 250,000g) was used as binding agent. For Pt CEs conductive transparent glass (FTO TEC 8, Pilkington Co) substrate was used. Dye sensitizer D719, cis-di-isothiocyanato-bis (2, 2'-bipyridyl 4,4'dicarboxylato) ruthenium (II) bis (tetra butyl ammonium) from Ever light Co was purchased. TiO₂ (P25 by Degussa Co) of 20 nm size was used for photo anodes. Ionomer surlyn of 60 μ m thickness purchased from solaronix. Other reagents were purchased from sigma Aldrich Co.

2.2 Fabrication of carbon fabric composite counter electrode

Different AC doped MWCNT nanostructures were synthesized in the following steps. The Schematic illustration of synthesis process given in Fig. S1 (supporting information). First of all, 1 mg mL^{-1} aqueous enzymatic solution of lipase enzyme was prepared in ethanol. 0.4 g of MWCNT was added in 100 mL enzymatic solution and stirred at room temperature for 8 hours. The enzymes were physically entrapped and adsorbed onto the MWCNT surface. Entrapped enzyme molecules substantially loosen the aggregation of MWCNT without compromising their electronic structures features. In the next step, different types of activated charcoal particles .i.e. coal, coconut shell, and Pine tree type were added into the individual MWCNT suspension and further dispersed for 8 hours. To facilitate the doping of activated charcoal into tubular graphitic structure of MWCNT, further 50 mL ethanol was added to dilute the suspension and ultrasonicated for at least 3 hours. Using ultra sonication, the large size charcoal particles break up and started induction into the MWCNT network. The suspension was vacuum filtered by using $0.5\ \mu\text{m}$ pore size PTFE polymer membrane filter. After that, the carbon filtrate washed two times with D.I water to remove any excess of non-adsorbed enzyme impurities. Next, the filtered and washed AC doped MWCNT cake was mixed with 15mL solution of carboxymethyl cellulose polymeric binder and grind in agate mortar to get consistent conductive carbon paste. The carbon paste was stored over night at room temperature for aging.

Cleaned polyester samples were cut into square and tape casted. AC doped MWCNT suspension was printed onto the polyester fabric via facile doctor blade technique under air drying (at $50\ ^\circ\text{C}$) method. The thickness of the layer was maintained by using 3M tape. The

counter electrodes were dried at 70 °C for 30 minutes, pressed at 130 °C for 20 minutes in hot press machine. Uncoated fabric edges were cut with scissor and 15×15 mm² square pieces were prepared for fabrication of cell. The final features of highly flexible textile fabric CE are shown in Fig. 1. For comparison, platinized FTO CEs were also prepared. 10 mM chloro platinic acid hexahydrate (H₂PtCl₆) solution was prepared in isopropanol and drop cast on FTO glass followed with annealing at 400 °C for 20 minutes.

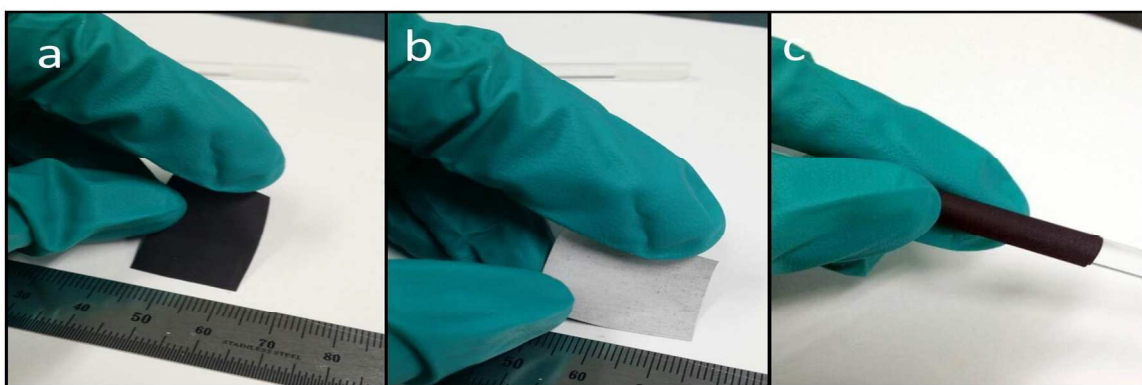


Fig. 1 Digital photo graphs of (a) front side, (b) back side (c) crack free flexible carbon fabric composite electrode.

2.3 Preparation of polymer gel electrolyte

In order to avoid the discharge of electrolyte through fabric weave, polymer gel electrolyte was used. For preparation 0.6 M 1-butyl-3-methyl-imidazolium iodide (BMII), 0.05 M iodine (I₂), 0.1 M lithium perchlorate (LiI), 0.1 M guanidine thiocyanate (GuNCS), 0.5 M 4-tert-butyl pyridine (TBP) and 5 wt% of polyethylene oxide polymer were dissolved in acetonitrile solution. Thick polymer gel electrolyte was injected from holed anode.

2.4 Cell fabrication

Photo anodes of SMT pattern were fabricated according to our previous research.^{31, 32} First of all, Holed FTO glass (15x15 mm²) were cleaned and treated with TiCl₄. 12 μm thick main layer (TiO₂, P25) and scattering layer of titania nanotubes (TNT) were deposited and sintered in consecutive steps of 70, 325, 375, 450, and 500°C for 30, 5, 5, 15, and 15 minutes, respectively. The annealed photo anodes were post treated with TiCl₄ and immersed in 0.3 mM solution of N719 for 12 hours. As shown in Fig. S2 (Supporting information), DSSCs were assembled with photo anode and carbon fabric composite CE, separated with polymer gel electrolyte in sandwich type arrangement using two 60μm thermoplastic hot-melt ionomer surlyn. The polymeric gel electrolyte was introduced from a holed photo anode by vacuum filling and sealed with surlyn and cover glass. The CE side of the cell was sealed by polymer film sheet.³³ The DSSCs with active area of 4x5 mm², measured by electronic microscope (Camscope, ICS-305B, sometech Co.) was used for photovoltaic test. For measuring the electrochemical characteristics of fabric CEs, identical dummy cells were assembled by two symmetrical carbon fabric CEs separated by polymer gel electrolyte. Polymer sheet films were attached on backside to stabilize the fabric cell. The symmetrical fabric cell was sealed in paraffin sheet pouch.

2.5 Characterization

The structural and surface morphology of carbon fabric composites were investigated by field emission-scanning electron microscope (FE-SEM, JEOL JSM-6700F) at an accelerating voltage of 15 kV. All carbon samples were coated with Pt for better structure image. The morphological characteristics of AC doped MWCNT samples were tested by transmission

electron microscope (TEM, JEOL JEM-2100F) at accelerating voltage of 200 kV. Surface area and pore size volume of different activated charcoal, MWCNT and AC doped MWCNT hybrid was measured with Perkin Elmer and Brunauer–Emmett–Teller data by using Quantachrome Autosorb-6 Sorption System. Wide angle X-ray diffraction (WAXD) was performed with a Rigaku Denki X-ray generator (Rigaku, D/MAX-2500), at 40 kV and 60 mA using Cu K α radiation ($\lambda=1.54181$ Å) radiation. The structural characteristics of different composite structure were investigated using Raman spectrometry (Jasco NRS-3100) with excitation wavelengths of 532 nm green laser. Further, surface characterization was done with XPS (X-ray photo spectroscopy) using a multi Lab ESCA 2000 system VG from Thermo Scientific, USA. For XPS, Mono-chromatized Al K α radiation with an energy step size of 0.05 eV was used. Fourier Transform infrared (FT-IR) spectra were also recorded using a Nicolett™ iS™ FT-IR spectrophotometer from Thermo Fisher Scientific Inc. (USA). All the fabric based samples were tested using the ATR Mode. Standard four point probe head system (RM 3000 resistivity test unit by Jandel engineering, Switzerland) was used to check the electrical conductivity of fabric CE. The electrical conductivity against flexibility of carbon fabric composites was tested using a custom-built two-probe device. The corrosion resistance of carbon coating (AC doped MWCNT) to electrolyte was recorded by UV-Vis spectrophotometer by using UV-1650 PC spectrophotometer (shamadzu Co.) in the wave length range of 350-800 nm. The fabric composite samples were immersed in electrolyte solution for 2 days and transmittance of electrolyte was recorded before and after immersion. Less transmittance change of electrolyte is an indication of better corrosion resistance. The cyclic voltammetry (CV) test was tested for different carbon fabric composites and carried out by using a three-electrode system in an argon-purged electrolyte (0.01 M LiClO₄, 10 mM LiI, and 1mM I₂ prepared in acetonitrile solution) at

a scan rate of 20 mV s^{-1} with ultimate electrochemical workstation (Bio Logic Co). The electrochemical properties of samples were measured by electrochemical impedance spectroscopy (EIS) by using symmetrical cell configuration. The photovoltaic performance of DSSCs fabricated with different CEs was evaluated using K101-Lab 20 source measuring unit (Mac Science Co). Solar simulator with 160 W Xenon arc lamp was used as light source (Spectral match; 0.75~1.25, non-uniformity of irradiance; $\leq \pm 2$ percentage, temporal instability; $\leq \pm 2\%$). The light intensity calibrated with a KIER-calibrated Si solar cell (Mc science Co). Photovoltaic parameters of the cells were measured under masked frame.

3. Results and discussion

3.1 Morphology and Structural characterization

Morphology of three types of activated charcoal is shown in Fig. S3 (supporting information). All ACs have amorphous structure and showed mesoporous surface. It can be seen that, Pine tree based AC has sharp board structure and defect rich structure. Whereas, coconut shell based AC has polygonal structure and lesser defects, while coal type AC has a round shape structure with low porous surface. Defect rich and porous morphology has advantage of fast triiodide reduction reaction and high diffusion of concentrated polymer electrolyte.

Fig. 2 shows the FE-SEM images of uncoated fabric and carbon coated fabric composite. It can be seen that, the surface of polyester fabric is relatively clean and smooth. After AC doped MWCNT printing, the surface of sample was fully covered with carbon sheet. There are no obvious cracks or flaws on the sheet were observed. Further high magnification (FE-SEM) image shows a three dimensional fragmented amorphous carbon sheets decorated with conductive

MWCNT network. Digital photograph showed the homogenous printing on textile substrate. Cross sectional view of Ac doped MWCNT hybrid coated on polyester weaved fabric was also observed. A thick mesoporous layer was observed on weaved pattern. The measured average thickness of the layer is about 16 μm , which is consistent with our previous studies.³⁴ Furthermore, energy dispersive spectroscopy (EDS) confirms the significant presence of carbon with high amount of oxygen in the carbon fabric composite. However, small Si peak confirmed the presence of hydrophobic surface finish shown in Fig. S4 (supporting information).

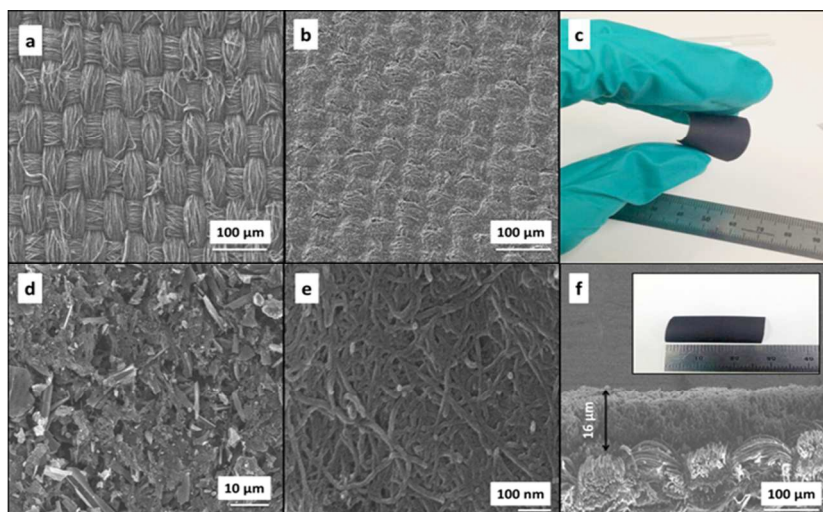


Fig. 2 FE-SEM images of (a) uncoated polyester fabric. (b) Ac doped MWCNT coated fabric. (c) Digital image of flexible carbon fabric composite. (d) Low magnification FE-SEM image of AC doped MWCNT. (e) High magnification FE-SEM image of AC doped MWCNT. (f) Cross-sectional FE-SEM image of carbon fabric composite (digital image of carbon fabric composite given in inset).

The AC doped MWCNT solutions were transferred onto the TEM grid for further characterization. From Fig. 3, it is observed that MWCNT are well dispersed with the lipase enzyme without apparent aggregation. TEM image also revealed the flat fragmented collapse of charcoal sheets decorated with CNT tubular network. The presence of charcoal particles along with MWCNTs can promote electron transfer from defect rich carbon to the MWCNT walls, decreasing the surface work function of MWCNT, thereby improving the reaction of I_3^- in reduction mechanism.

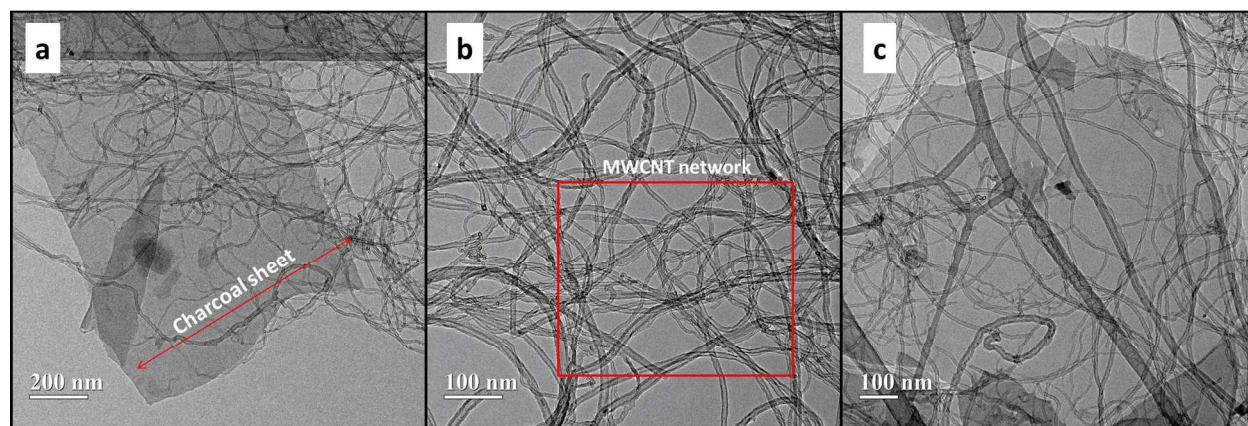


Fig. 3 TEM images of Ac doped MWCNT hybrid

To further characterize the identity and structure of different types of carbon fabric composites, WXR, Raman, XPS and FT-IR tests were performed. Fig. 4a showed the WXR spectrum of carbon fabric composite prepared with different types (i.e. coal, coconut shell and pine tree) of charcoal particles. In case of composite C, a sharp diffraction peak centered at 25.8° can be indexed to (002) reflection of the graphitic carbon of MWCNT.³⁵ In addition, the XRD pattern also showed peak at 48.05° showed the presence of amorphous charcoal. The small

diffraction peaks centered at 33.03° indexed to (111) reflection of silicon peak can be assigned as the contribution of hydrophobic surface finish on polyester fabric.³⁶ Very small peak centered at 37.50° indicate the presence of cellulosic content of CMC polymeric binder. The wide diffraction peak centered at 22.68° showed the presence of polymeric chain of polyester fabric.

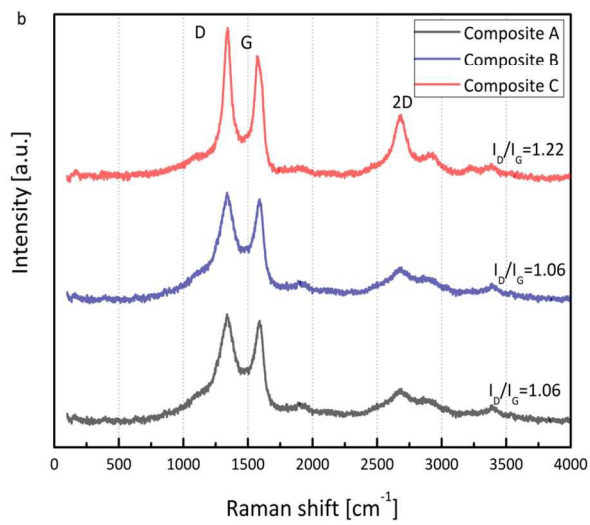
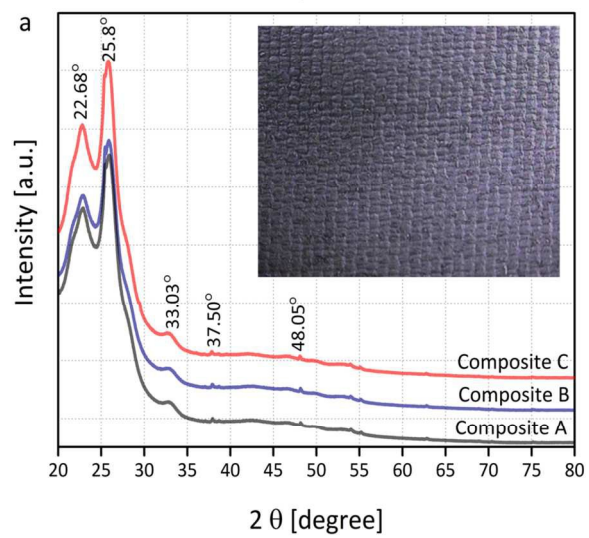
Raman spectra of Carbon fabric composite synthesized with different charcoal shown in Fig. 4b. A relatively higher D band for composite C (pine tree) was revealed due to high defect produced by amorphous carbon. The intensity ratio of the crystalline G and defect rich D bands (I_D/I_G) in the Raman spectra is related to the sp^2 carbon cluster sizes in the structure and is nearly proportional to the defect density. However, I_D/I_G ratio ($I_D/I_G=1.22$) indicates that composite C consist of partial mesoporous carbon with ordered MWCNT structure, responsible for high conductivity and electro catalytic activity of composite C electrode. Further Raman spectra of as synthesized AC doped MWCNT is given in Fig. S5 (supporting information). A relatively higher D band for the AC doped MWCNT than that of MWCNT was revealed due to structural distortion caused by doping of amorphous charcoal particles.

The XPS survey spectrum of carbon fabric composite shows a pre-dominant carbon peak C1 at 284.4 eV, along with high amount of oxygen O1 at 534.8 eV, possibly due to incorporation of oxygen containing defect rich charcoal colloid. The survey XPS spectrum of CNT coated fabric and AC doped MWCNT coated fabric shown in Fig. S6 (supporting information). Meanwhile, the C1s core-level spectrum (Fig. 4c) of the AC doped MWCNT could be fitted into four component peaks with binding energies of 284.4, 284.9, 287.0 and 294.0 eV, due to the sp^2 hybridized carbon, sp^3 hybridized carbon, C–O and π - π interactions, respectively. Moreover, the O1s spectrum shown in Fig. 4d could be fitted into two component peaks with binding energies of 531.8 and 533.9 eV, due to the contribution of C-O and C=O, respectively. The oxygenated

carbons were also detected in the XPS spectrum of AC doped MWCNT. However, the intensities of these peaks readily increased from those of MWCNT, which indicates that amorphous carbon were successful doped into CNT tubular rings.

To determine the type and amount of surface functional groups in coal, coconut shell and pine tree type activated charcoal are determined by FT-IR. Surface functional groups in activated charcoal have been identified and analyzed using charcoal dispersions in potassium bromide (KBr). Different oxygen functional groups on activated charcoal strongly influence the absorptive behavior, and catalytic reduction of charcoal. FT-IR spectrum of different charcoal is shown in Fig. S7 (supporting information). The C–OH stretching mode and the bending mode can be found at 3445 and 1635, respectively. Therefore, we can reasonably assume that this bond is probably located in the carbon matrix³⁷. High absorbance spectra of C-OH bond in pine tree charcoal indicate its absorptive properties.

Further FTIR-ATR spectrum for polyester fabric and carbon fabric composite was also recorded. The FT-IR spectrum of carbon fabric shown in Figure S8 (supporting information) indicates no change in the spectrum when compared with bare polyester fabric. The modification in the spectra is directly related to the chemical reaction of carbon layer with polyester fabric. FTIR-ATR investigation specified that no chemical reaction other than physical adhesion took place between carbon and polyester fabric.



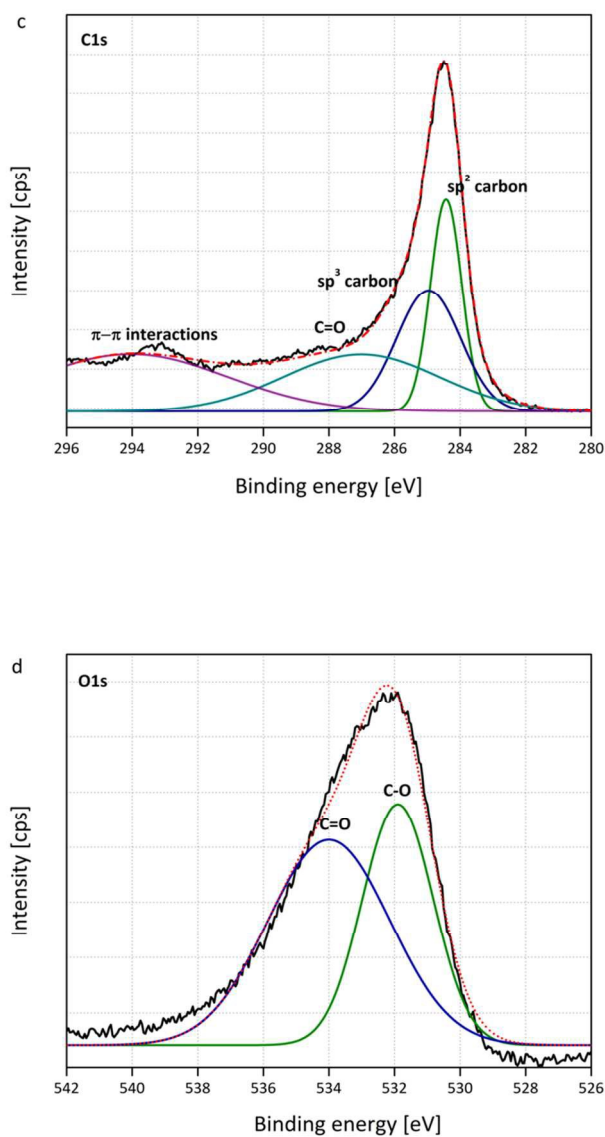


Fig. 4 (a) XRD spectrum of carbon fabric composites. (b) Raman spectrum of carbon fabric composites. (c) De convoluted C1s spectra for carbon fabric composite. (d) De convoluted O1s spectra for carbon fabric composite.

3.2 Surface area and porosity

To investigate the surface area and porosity of AC doped MWCNT hybrid, N₂ adsorption–desorption isotherm and the pore size was observed. The as-synthesized carbon layer exhibited typical N₂ hysteresis of adsorption-desorption curves shown in Fig. S9 (supporting information), indicating the characteristic of amorphous carbon. As compare to AC free MWCNT, AC doped MWCNT showed higher amount of N₂ absorption at high relative pressure, signifying the presence of high mesoporous carbon in the substrate. AC doped MWCNT have higher specific surface area of 500.0965 m² g⁻¹, with 1.102288 cm³ g⁻¹ pore volume, whereas AC free MWCNT have low specific surface area of 337.1920 m² g⁻¹ with 1.030778 cm³ g⁻¹ pore volume. High specific surface area and pore volume structure will provide more accessibility to the I₃⁻ ions, and improved electro catalytic activity³⁸. Surface area and pore volume of three types of activated charcoal (coal, Coconut shell and pine tree) given in Table. 1. Pine tree type activated carbon has high pore size volume with high surface area, responsible for its efficient performance.

Table 1. Characteristics of different activated charcoal.

Properties	Coal	Coconut shell	Pine tree
S _{BET}	754.1050	1,111.3174	963.0311
Pore volume	0.434079	0.523684	0.636723

3.3 Electrical conductivity and stability

The sheet resistance of AC doped MWCNT coated fabric measured by four point probe showed excellent conductivity of $12 \Omega \text{ sq}^{-1}$ when prepared with pine tree based charcoal. These results can be comparable to that of platinized FTO glass of $8 \Omega \text{ sq}^{-1}$. Sheet resistance of different fabric composites listed in Table.2-Table.4, respectively. Ac doped MWCNT was selected as the conducting electro catalytic material on fabric, as it has significantly good catalytic reaction with iodide electrolytes and can easily be coated on fabrics at relatively low temperature. In order to test the conductivity of textile CE against different bending positions, a custom-built two-probe device with slide clamps was build. Sample size of 1×3 cm was bent gradually in different positions and its electrical conductivity was measured shown in Fig.S10 (supporting information). Fabric electrode showed negligible difference in conductivity over different positions shown in Fig. S11a (supporting information). Conductivity of fabric electrode against bending cycles was also measured. The variation in the electrical resistance of the fabric was negligible over 10 bending cycles. After the bending test, no cracks were observed on the coated fabric Fig. S11b (supporting information).

In order to test the corrosion resistance of carbon composite fabrics to electrolyte, the samples were immersed in electrolyte solution for two days and transmittance of electrolytes was noted. The transmittance of electrolytes did not change remarkably after immersion of the coated fabrics (Fig. 5). The surface coating of immersed samples was stable, no obvious cracking or imperfections were observed.

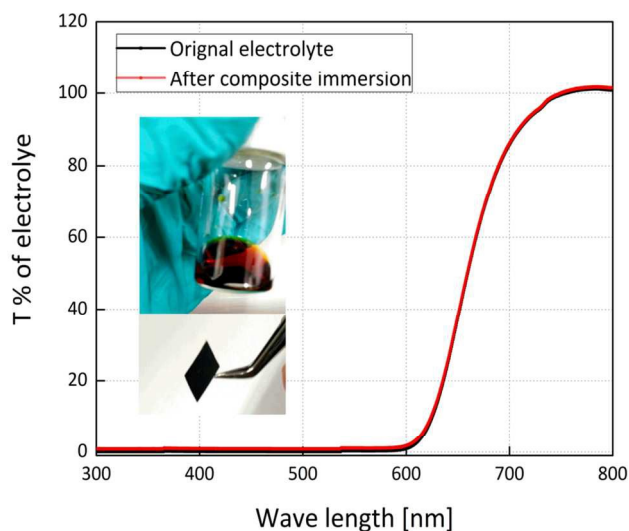


Fig. 5 Transmittance of electrolytes before and after immersion of fabric sample (inset shows the Immersion in electrolyte and stable carbon coating).

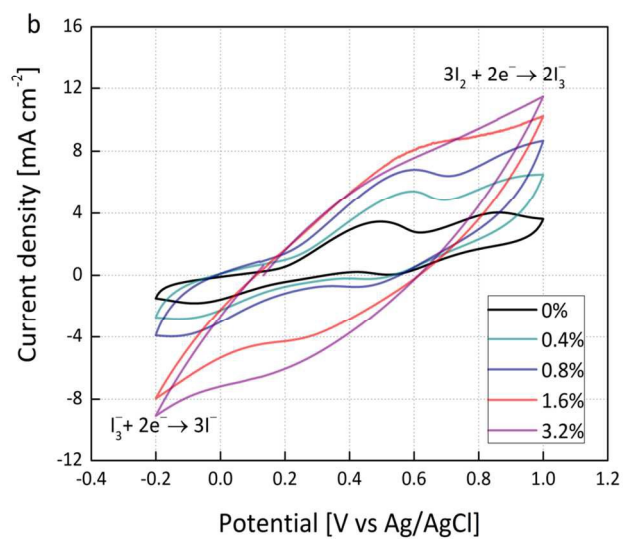
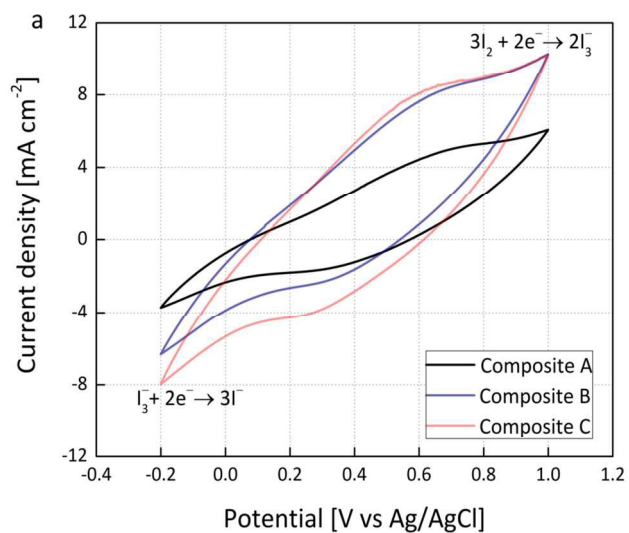
3.4. Electro catalytic activity

The electro catalytic activity of the CE is a significantly parameter for improving the performance of DSSCs. Therefore, electro catalytic activities of the different carbon fabric composites were initially studied by the cyclic voltammetry (CV) technique. AC doped MWCNT hybrid printed on polyester fabric are expected to produce high conductivity and electro catalytic activity (ECA) towards the reduction of I_3^- . The CV curves of fabric CEs using a three-electrode system are presented in Fig. 6a. Two distinctive oxidation and reduction peaks were observed for different fabric composites. The negative pair was assigned to the reduction reaction (eq.1) and the positive one was assigned to the oxidation reaction (eq. 2).³⁹



The three important parameters which determine the catalytic activity of the CE are cathodic peak potential (E_{CP}), cathodic current density (I_{PC}), and the peak to peak separation (E_{pp}) of potential difference. It indicates that a higher I_{PC} , a more positive E_{CP} and a lower E_{pp} value demonstrate the greater electro catalytic activity of CE⁴⁰. It was observed that, the variation of different carbon content around MWCNT, caused variance in electro catalytic activity (ECA) of the fabric electrode. It can be seen that, the carbon fabric composite synthesized with composite C has larger oxidation and reduction current densities as compare to composite A, and Composite B, respectively. These results ascribed to the high surface area and pore volume of pine tree type charcoal, which affect its electro catalytic activity⁴¹. The cathodic peak potential (-2.43V) and larger cathodic current density (-7.945 mA cm⁻²) indicate its superior electrical conductivity and electro catalytic activity for I_3^- reduction. Fig. 6b shows the CVs of carbon fabric electrodes prepared with different charcoal content. It was interesting to find out that, by increasing the charcoal content high electro catalytic activity was observed. AC free CNT coated fabric possess low ECA with (1.95 mA cm⁻²), whereas 0.8 wt% AC fabric electrode have large cathodic current density with (4.09 mA cm⁻²) The profile and peak location of CV for the carbon fabric (0.8 wt%) electrode is similar to Pt coated FTO glass, demonstrating synchronized features of high catalytic activity and conductivity. Furthermore, by increasing the AC content from 1.6 wt% to 3.2 wt%, CV profile is changed to pure activated carbon. Low ECA with only one reduction peak was observed in high charcoal content.⁴² It was confirmed that, our suggested carbon fabric composite (0.8 wt%) shows higher ECA than conventional platinized

FTO glass showed an E_{pp} of 0.70 V which is comparable with Pt catalyst with 0.24 V E_{pp} indicating difference of ECA of fabric and Pt CE (Fig. 6c).



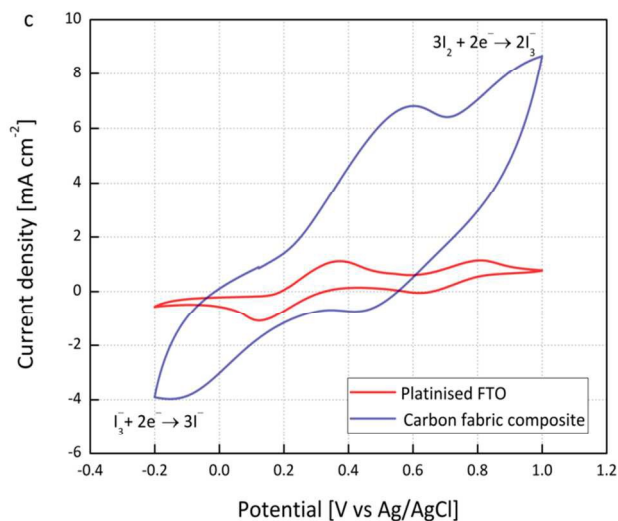
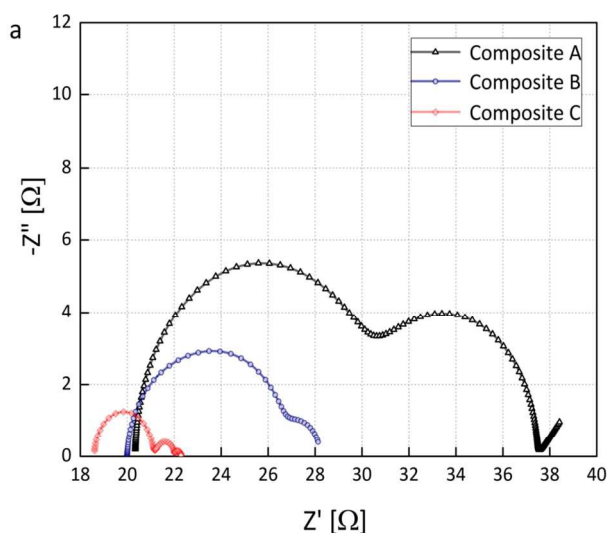


Fig. 6 Cyclic voltammograms of iodide species for (a) Different carbon fabric composites. (b) Effect of wt% of charcoal on ECA. (c) Pt and carbon fabric composites (0.8 wt%).

3.5 Electrochemical properties

To understand the electrochemical catalytic activity of three kinds of carbon fabric CE, electrochemical impedance spectroscopy (EIS) were carried out. In EIS characterization, electrochemical reaction rates of redox couple (I^-/I_3^-) were measured with electrochemical impedance spectroscopy (EIS) with symmetrical cells as reported in the previous literature^{43,44}. The symmetrical cell configuration shown in Fig. S12 (supporting information), comprising two identical carbon fabric electrodes, used to calculate the charge transfer reaction processes at the interface between CE and polymer gel electrolyte. The sheet resistance (R_S) and (R_{CT}) parameters were obtained by fitting EIS plots using a Randles-type equivalent circuit in EC-lab software shown in Fig. S13 (supporting information). The typical Nyquist plots of symmetrical cells are shown in Fig. 7a. The plot shows a well-defined semicircle with one small semi-circle.

The high frequency (around 100 kHz) intercept on the real axis represents the series resistance (R_S) of the electrode. The first semicircle at the medium frequency region is related to the charge transfer resistance (R_{CT}) and the corresponding constant phase element (CPE) of counter electrodes and electrolyte interface reaction, while the other small semicircle at low frequency region demonstrates the Nernst diffusion impedance (Z_W) of (I^-/I_3^-) in the electrolyte. since the Nernst diffusion impedance is negligible for our focus therefore, we mainly emphasis on the R_S and R_{CT} of CEs. The R_S and R_{CT} of different CEs together with other parameters are tabulated in Table. 2.



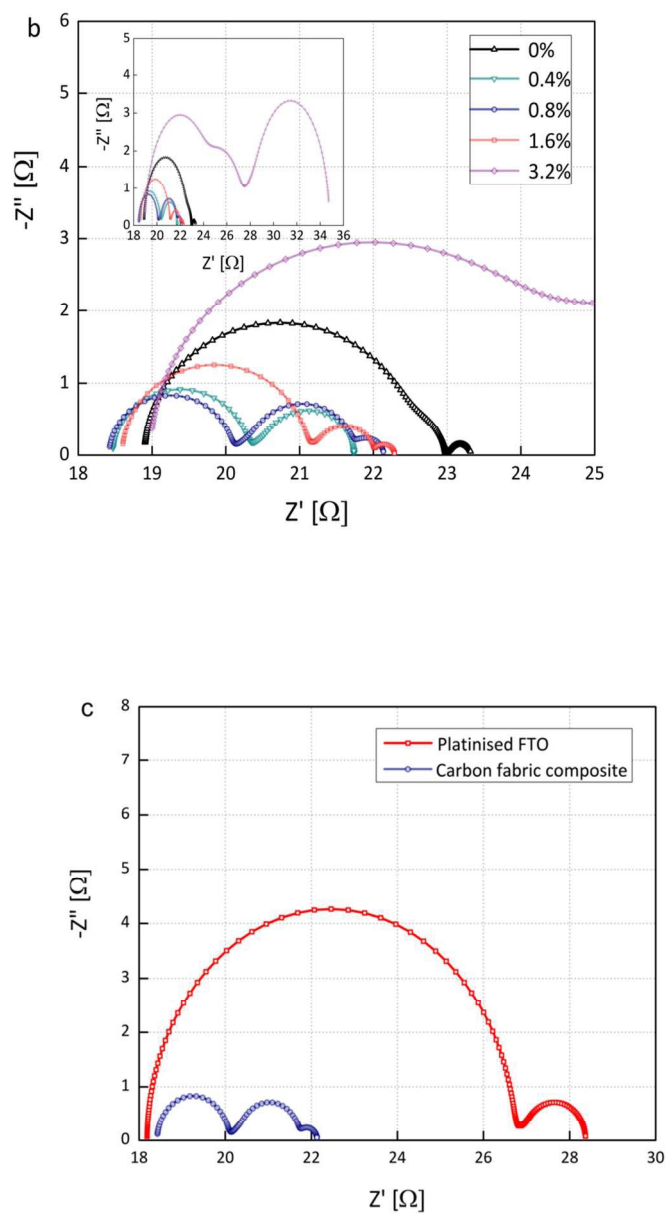


Fig. 7 Nyquist plot for (a) carbon fabric composite fabricated with coal, coconut shells, and pine tree charcoal (1.6 wt%).(b) Effect of wt% of charcoal on R_{CT} . (c) Pt and carbon fabric composite (0.8 wt%).

The R_S of three electrodes are negligibly varied, demonstrating good bonding strength of carbon sheet with textile fabric. According to the values obtained from the Nyquist plot, The R_{CT} of Composite C (pine tree type) electrode was found to be 2.40 Ω , indicating a high electrochemical activity and conductivity than its counter parts. The R_{CT} value of composite A and composite B has comparatively high R_{CT} of 6.50 and 2.55 Ω , respectively. This can be attributed to slow ionic diffusion in the porous structure of Ac doped MWCNT hybrid synthesized with coal and coconut shell type charcoal. The above results confirm the significance of defect rich pine tree type charcoal in the catalytic reduction mechanism.

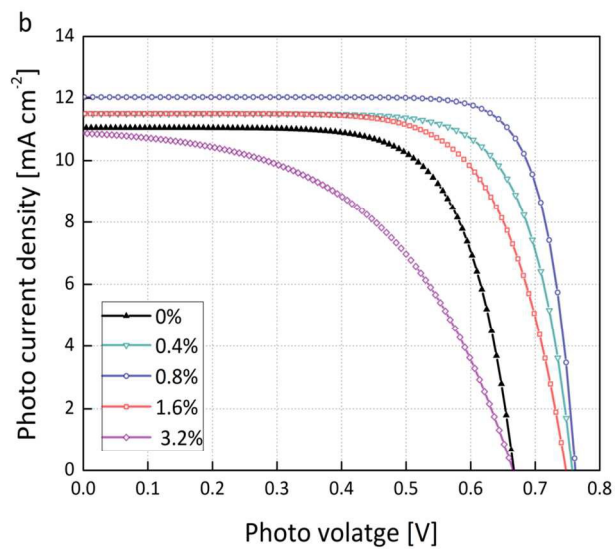
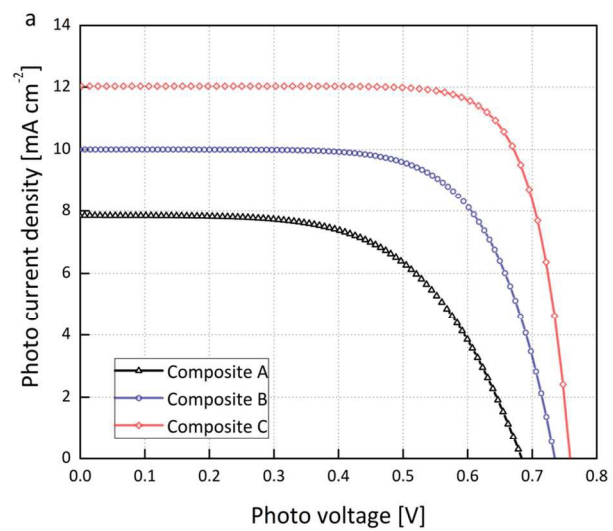
To further optimize the interfacial charge transfer process between polymer gel electrolyte and composite C CEs, different composite C electrodes were fabricated by altering the charcoal content. The R_{CT} of composite C electrode decreases gradually with increasing charcoal content from 0 wt% to 0.8 wt%. This effect due to the high porosity embedded in MWCNT. In brief, carbon electrode of 0.8 wt% AC, highlighting a reduction in R_{CT} with 1.38 Ω (Fig. 7b). This proves that the synchronized effect of MWCNT with appropriate dosage of activated charcoal can enhance charge transfer mechanism of CEs when used with gel electrolyte. Further increment in charcoal content, high R_{CT} and low sheet to substrate adhesion was observed, which may be due to mismatch composite ratio. The composite C fabricated with 0.8 wt% pine tree can be compared to platinized FTO glass (Fig. 7c). The R_S of the carbon fabric is comparable with Pt electrode due to the optimization of doping process which enhances the conductivity of fabric CE. The R_{CT} value of Pt is 8.55 Ω , which is much higher as compared to carbon fabric CE (1.38 Ω). This result further confirms that carbon fabric composite consist of highly conductivity and porous structure, which enhance the charge transfer kinetics and entrap large amount of gel electrolyte for faster tri-iodide reduction. As the faster charge transfer

mechanism improved by carbon fabric also helps to sustain maximum current attainable in DSSCs. Therefore, low R_S and R_{CT} of composite C CE are responsible for the high FF and J_{SC} of the corresponding DSSCs, listed in Table 3 and Table 4, respectively.

3.6 Photo voltaic data

For feasible fabrication of textile fabric CE, we choose polymer gel electrolyte and FTO based photo anodes to fabricate DSSCs. The photo current-voltage (I-V) curves of DSSCs based on different carbon fabric CEs measured under a simulated AM 1.5 illuminations (1 sun, 100 $mW\ cm^{-2}$). Fig. 8a shows the photocurrent density-voltage (I-V) curves of DSSCs based on composite A (coal), Composite B (coconut shell), Composite C (pine tree) CEs, respectively. Detailed photovoltaic parameters are summarized in Table 2.

DSSCs based on Composite A CE, exhibited poor performance with low values of FF and PCE, only 60.38% and 3.31%, respectively. The V_{OC} and FF are largely affected by electro catalytic activity of the CE. While low J_{SC} obtained is due to low conductivity of coal based Composites. When using the Composite B, significant photovoltaic improvements were achieved, presenting a FF and PCE of 67.86% and 5.03%, respectively. Furthermore, using Composite C CE, a noticeable improvement in FF and PCE was observed with 69.87% and 5.97%. Except for FF, the increases in short-circuit current density (J_{SC}) and open-circuit voltage (V_{OC}) are also observed. This result confirms that, pine tree type charcoal materials are more electro catalytic active than its counter parts and more suitable for CNT doping. Due to their highly porous and defect rich nature, composite C structures acquires the best photovoltaic parameters.



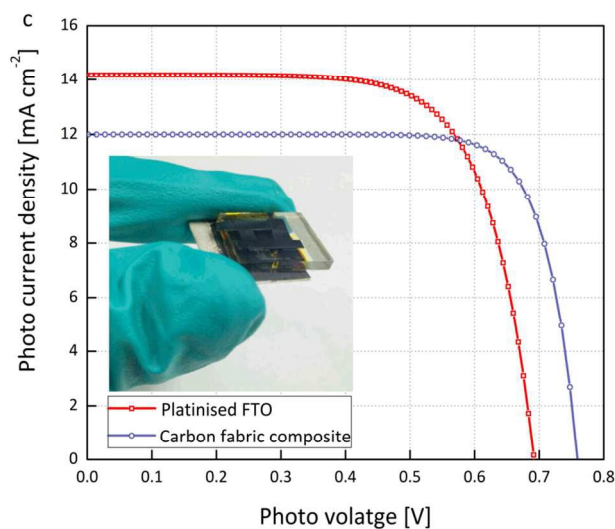


Fig. 8 (a) Photo voltaic performances of DSSCs based on three types of carbon fabric composites CEs. (b) Effect of wt% of charcoal on photovoltaic performance. (c) Comparison of photovoltaic performance of DSSCs fabricated with Pt and carbon fabric CE (Inset shows the digital photo graph of DSSCs fabricated with carbon fabric CE).

Carbon nanotubes are highly conductive, but less electro catalytic active due to low surface area and porosity.^{45, 46} To speed up kinetics of (I^-/I_3^-) activated charcoal particles (AC) were doped with carbon nanotube to integrate porosity and defects. We tried to add 0.4, 0.8, 1.6, and 3.2 wt% of AC into MWCNT dispersion, and obtained the synchronized effects of conductive CNT and defect rich AC. Fig. 8b presents the I–V curves of the DSSCs based on carbon fabric CEs containing different wt% of AC. It is shown in Table 3, with the addition of AC, the efficiency first increased and then decreased. The short current density (J_{SC}) and fill factor (FF) show the same change tendency. The DSSC using the AC doped MWCNT CE containing 0.8 wt% of AC reaches an efficiency of 7.29%, with high FF of 79.03%. However, when we added over 0.8 wt% of AC, catalytic activities of the CEs started to decline due to high

defects produced by the AC, might lower the charge sites for iodide (I^-) reduction and thus reduces the FF and J_{SC} of cell. Low sheet adhesion was also observed in high charcoal dosage. For instance, cell using the CE comprising 3.2 wt% of AC yields a low efficiency of 3.61 %.

Fig. 8c presents the I–V curves of the DSSCs based on platinized FTO glass and carbon fabric CEs. The inset shows the Fabricated DSSCs based on fabric CE. The CE is composed of carbon layer printed on woven fabric. The results are tabulated in Table 4. The cell fabricated with the conventional platinized FTO glass resulted in 7.16% efficiency; whereas, the cell prepared with fabric CE reached 7.29% efficiency, outperforming platinized FTO electrode. This result corresponds to among the highly efficient dye sensitized solar cells based on fabric based CE. Specifically, both the open circuit voltage (V_{OC}) and fill factor (FF) were found to increase for the fabric based DSSC. As per previous investigation of EIS analysis, the optimized induction of activated charcoal into MWCNT displayed a defect rich and porous conductive structure with improved adhesion to the textile substrate led to enhance conductivity and electrochemical properties. This effect essentially directed to an increase of the electron transport at the interface of AC doped MWCNT and polymer electrolyte. Hence, high electro catalytic activity, reduction of the interfacial resistance (R_{CT}) resulting in a high photo voltage (V_{OC}), and FF.⁴⁷ Low J_{SC} of carbon fabric composite was concealed with high V_{OC} and FF values. However, low current density (J_{SC}) suggests the difference of light harvesting properties of different CEs.⁴⁸

Table 2. Electrochemical and photovoltaic performance of DSSCs fabricated with different carbon fabric composites.

Type of composite	Electrode	Symmetrical cell			DSSC		
	Resistivity	R_s	R_{CT}	J_{sc}	V_{oc}	FF	PCE
	($\Omega \text{ sq}^{-1}$)	(Ω)	(Ω)	(mA cm^{-2})	(V)	(%)	(%)
Composite A	15.5	20.34	6.50	8.06	0.681	60.38	3.31
Composite B	13.1	19.95	3.94	10.09	0.735	67.86	5.03
Composite C	12.5	18.60	2.40	11.50	0.743	69.87	5.97

Table 3. Electrochemical and photovoltaic performance of DSSCs fabricated with carbon fabric composites of different wt% of activated carbon (pine type).

wt% of carbon	Electrode	Symmetrical cell			DSSC		
	Resistivity	R_s	R_{CT}	J_{sc}	V_{oc}	FF	PCE
	($\Omega \text{ sq}^{-1}$)	(Ω)	(Ω)	(mA cm^{-2})	(V)	(%)	(%)
0	15.5	18.91	3.58	11.05	0.673	70.45	5.24
0.4	13.3	18.48	1.82	11.52	0.769	73.98	6.56
0.8	12.1	18.40	1.38	12.03	0.766	79.03	7.29
1.6	12.5	18.60	2.40	11.50	0.743	69.87	5.97
3.2	15.8	19.01	5.71	11.03	0.665	49.12	3.61

Table 4. Comparison of electrochemical and photovoltaic performance of DSSCs fabricated with platinized FTO glass and carbon fabric composite CEs.

CEs	Electrode	Symmetrical cell			DSSC		
	Resistivity	R_s	R_{CT}	J_{sc}	V_{oc}	FF	PCE
	($\Omega \text{ sq}^{-1}$)	(Ω)	(Ω)	(mA cm^{-2})	(V)	(%)	(%)
Platinized FTO	8.0	18.10	8.55	14.184	0.701	72.06	7.16
Carbon fabric	12.1	18.40	1.38	12.03	0.766	79.03	7.29

Conclusion

In summary, highly efficient and flexible counter electrode was successfully developed by a facile approach to fabricate an AC doped MWCNT hybrid printed on woven polyester fabric. Initially, three different types of charcoal (coal, coconut shell, and pine tree) were doped with MWCNT and printed on polyester fabric. It has been proven that, pine tree composite (composite C) is compatible for the fabrication of highly porous and defect rich hybrid structure and recommended for textile fabric coating. Optimization of doping with different dosage of charcoal in MWCNT, also improve the conductivity and electro catalytic activity of fabric CE. Finally, the efficiency of our suggested DSSCs using textile fabric CE achieved 7.29% efficiency, outperforming platinized FTO glass. The whole design and fabrication is low cost and commercially feasible. Therefore, it can estimate that this novel textile fabric CE will be promising for the roll to roll production of flexible textile structured solar cell.

References

1. W.-w. Liu, X.-b. Yan, J.-w. Lang, C. Peng and Q.-j. Xue, *Journal of Materials Chemistry*, 2012, 22, 17245-17253.
2. N. A. Alhebshi, R. B. Rakhi and H. N. Alshareef, *Journal of Materials Chemistry A*, 2013, 1, 14897-14903.
3. X. Cheng, X. Fang, P. Chen, S.-G. Doo, I. H. Son, X. Huang, Y. Zhang, W. Weng, Z. Zhang, J. Deng, X. Sun and H. Peng, *Journal of Materials Chemistry A*, 2015, 3, 19304-19309.
4. Y. Xie, Y. Liu, Y. Zhao, Y. H. Tsang, S. P. Lau, H. Huang and Y. Chai, *Journal of Materials Chemistry A*, 2014, 2, 9142-9149.
5. Y. Zhu, F. Wang, L. Liu, S. Xiao, Z. Chang and Y. Wu, *Energy & Environmental Science*, 2013, 6, 618-624.
6. B. Wang, S. Li, X. Wu, B. Li, J. Liu and M. Yu, *Physical Chemistry Chemical Physics*, 2015, 17, 21476-21484.
7. M. Li, X. Wang, Y. Wang, B. Chen, Y. Wu and R. Holze, *RSC Advances*, 2015, 5, 52382-52387.
8. K. Jost, C. R. Perez, J. K. McDonough, V. Presser, M. Heon, G. Dion and Y. Gogotsi, *Energy & Environmental Science*, 2011, 4, 5060-5067.
9. J.-W. Jeon, S. R. Kwon and J. L. Lutkenhaus, *Journal of Materials Chemistry A*, 2015, 3, 3757-3767.
10. S. Pan, Z. Yang, P. Chen, J. Deng, H. Li and H. Peng, *Angewandte Chemie*, 2014, 126, 6224-6228.
11. S. Pan, Z. Yang, H. Li, L. Qiu, H. Sun and H. Peng, *Journal of the American Chemical Society*, 2013, 135, 10622-10625.
12. T. Chen, L. Qiu, Z. Yang, Z. Cai, J. Ren, H. Li, H. Lin, X. Sun and H. Peng, *Angewandte Chemie International Edition*, 2012, 51, 11977-11980.
13. K. Jost, G. Dion and Y. Gogotsi, *Journal of Materials Chemistry A*, 2014, 2, 10776-10787.
14. T. M. Brown, F. De Rossi, F. Di Giacomo, G. Mincuzzi, V. Zardetto, A. Reale and A. Di Carlo, *Journal of Materials Chemistry A*, 2014, 2, 10788-10817.
15. T. Chen, L. Qiu, H. G. Kia, Z. Yang and H. Peng, *Advanced Materials*, 2012, 24, 4623-4628.
16. S. Mathew, A. Yella, P. Gao, R. Humphry-Baker, F. E. Curchod, N. Ashari-Astani, I. Tavernelli, U. Rothlisberger, K. Nazeeruddin and M. Grätzel, *Nat Chem*, 2014, 6, 242-247.
17. B. O'regan and M. Grätzel, *nature*, 1991, 353, 737-740.
18. S. J. Lue, P. W. Lo, L.-Y. Hung and Y. L. Tung, *J Power Sources*, 2010, 195, 7677-7683.
19. K. SeokáLee, H. KenáLee, D. HwanáWang, J. YoungáLee, O. OkáPark and J. HyeokáPark, *Chemical communications*, 2010, 46, 4505-4507.
20. X. Cai, S. Hou, H. Wu, Z. Lv, Y. Fu, D. Wang, C. Zhang, H. Kafafy, Z. Chu and D. Zou, *Physical Chemistry Chemical Physics*, 2012, 14, 125-130.
21. M. Janani, P. Srikrishnarka, S. V. Nair and A. S. Nair, *Journal of Materials Chemistry A*, 2015, 3, 17914-17938.

22. M. Tathavadekar, M. Biswal, S. Agarkar, L. Giribabu and S. Ogale, *Electrochimica Acta*, 2014, 123, 248-253.
23. I. A. Sahito, K. C. Sun, A. A. Arbab, M. B. Qadir and S. H. Jeong, *Electrochimica Acta*, 2015, 173, 164-171.
24. T. Chen, L. Qiu, Z. Cai, F. Gong, Z. Yang, Z. Wang and H. Peng, *Nano letters*, 2012, 12, 2568-2572.
25. J. Velten, Z. Kuanyshbekova, Ö. Göktepe, F. Göktepe and A. Zakhidov, *Applied Physics Letters*, 2013, 102, 203902.
26. Y. Yang, J. Xiao, H. Wei, L. Zhu, D. Li, Y. Luo, H. Wu and Q. Meng, *RSC Advances*, 2014, 4, 52825-52830.
27. W. J. Lee, E. Ramasamy, D. Y. Lee and J. S. Song, *ACS applied materials & interfaces*, 2009, 1, 1145-1149.
28. B. Lu, Z. Xiao, H. Zhu, W. Xiao, W. Wu and D. Wang, *J Power Sources*, 2015, 298, 74-82.
29. D. Saha, Y. Li, Z. Bi, J. Chen, J. K. Keum, D. K. Hensley, H. A. Grappe, H. M. Meyer III, S. Dai and M. P. Paranthaman, *Langmuir*, 2014, 30, 900-910.
30. A. A. Arbab, K. C. Sun, I. A. Sahito, M. B. Qadir and S. H. Jeong, *Applied Surface Science*, 2015.
31. K. C. Sun, M. B. Qadir and S. H. Jeong, *RSC Advances*, 2014, 4, 23223-23230.
32. M. B. Qadir, K. C. Sun, I. A. Sahito, A. A. Arbab, B. J. Choi, S. C. Yi and S. H. Jeong, *Solar Energy Materials and Solar Cells*, 2015, 140, 141-149.
33. J. Xu, M. Li, L. Wu, Y. Sun, L. Zhu, S. Gu, L. Liu, Z. Bai, D. Fang and W. Xu, *J Power Sources*, 2014, 257, 230-236.
34. A. A. Arbab, K. C. Sun, I. A. Sahito, M. B. Qadir and S. H. Jeong, *Physical Chemistry Chemical Physics*, 2015, 17, 12957-12969.
35. B. Lee, D. B. Buchholz and R. Chang, *Energy & Environmental Science*, 2012, 5, 6941-6952.
36. T. Hatchard and J. Dahn, *Journal of The Electrochemical Society*, 2004, 151, A838-A842.
37. J. Romanos, M. Beckner, T. Rash, L. Firlej, B. Kuchta, P. Yu, G. Suppes, C. Wexler and P. Pfeifer, *Nanotechnology*, 2012, 23, 015401.
38. S. I. Cha, B. Koo, S. Seo and D. Y. Lee, *J. Mater. Chem.*, 2010, 20, 659-662.
39. Y. Li, H. Wang, H. Zhang, P. Liu, Y. Wang, W. Fang, H. Yang, Y. Li and H. Zhao, *Chemical Communications*, 2014, 50, 5569-5571.
40. J. T. Park, C. S. Lee and J. H. Kim, *Nanoscale*, 2015, 7, 670-678.
41. C. H. Yoon, S. K. Chul, H. H. Ko, S. Yi and S. H. Jeong, *Journal of nanoscience and nanotechnology*, 2013, 13, 7875-7879.
42. G. Yue, J. Wu, Y. Xiao, M. Huang, J. Lin and J.-Y. Lin, *Journal of Materials Chemistry A*, 2013, 1, 1495-1501.
43. H. Bi, H. Cui, T. Lin and F. Huang, *Carbon*, 2015, 91, 153-160.
44. F. Gong, X. Xu, Z. Li, G. Zhou and Z.-S. Wang, *Chemical Communications*, 2013, 49, 1437-1439.
45. K. Suzuki, M. Yamaguchi, M. Kumagai and S. Yanagida, *Chemistry Letters*, 2003, 32, 28-29.
46. L. Y. Heng, A. Chou, J. Yu, Y. Chen and J. J. Gooding, *Electrochemistry communications*, 2005, 7, 1457-1462.

47. P. Dong, Y. Zhu, J. Zhang, F. Hao, J. Wu, S. Lei, H. Lin, R. H. Hauge, J. M. Tour and J. Lou, *Journal of Materials Chemistry A*, 2014, 2, 20902-20907.
48. B. Lee, D. B. Buchholz and R. P. H. Chang, *Energy & Environmental Science*, 2012, 5, 6941-6952.

Graphical Abstract

